Buckling of actin-coated membranes under application of a local force

Helfer, E.; Harlepp, S.; Bourdieu, L.; Robert, J.; MacKintosh, F.C.; Chateney, D.

Published in:
Physical Review Letters

Buckling of Actin-Coated Membranes under Application of a Local Force

E. Helfer,[1,*] S. Harlepp,[1] L. Bourdieu,[1,†] J. Robert,[1] F. C. MacKintosh,[1,2,‡] and D. Chatenay[1]

[1]*Laboratoire de Dynamique des Fluides Complexes, U.M.R. C.N.R.S. 7506, Strasbourg, France*

[2]*Department of Physics, University of Michigan, Ann Arbor, Michigan*

(Received 13 February 2001; published 6 August 2001)

The mechanical properties of composite membranes obtained by self-assembly of actin filaments with giant fluid vesicles are studied by micromanipulation with optical tweezers. These complexes exhibit typical mechanical features of a solid shell, including a finite in-plane shear elastic modulus ($\sim 10^{-6}$ N/m). A buckling instability is observed when a localized force of the order of 0.5 pN is applied perpendicular to the membrane plane. Although predicted for polymerized vesicles, this is the first evidence of such an instability.

DOI: 10.1103/PhysRevLett.87.088103 PACS numbers: 87.19.Tt, 68.03.–g, 82.65.+r, 87.80.–y

Solid, tethered, or polymerized membranes have been studied in detail over the years from the theoretical point of view [1–4]. They exhibit rich fluctuation properties and have been viewed as simple mechanical models of cells plasma membrane. Red blood cells, for example, possess a two-dimensional (2D) cross-linked spectrin network, underlying the lipid membrane, partly responsible for their equilibrium shapes, mechanical properties, and thermal shape fluctuations [5–7]. Similarly, in many eukaryotic cells, a thick actin cortex associated with the plasma membrane is partly responsible for cell shape and mechanical properties [7]. From a physical point of view, membranes can be considered as thin elastic shells of thickness h, with a bending modulus κ, an in-plane shear modulus μ, and an in-plane stretching modulus K [1–5]. The bending modulus is usually very small in these systems. Therefore the in-plane strain energies are much larger than the bending energy and pure bending deformations are energetically favorable. However, whereas the in-plane strain is second order in bending amplitudes for flat membranes [8], for curved shells the situation is different [8]. For a spherical shell whose radius R is increased to a radius $R + \xi$, the in-plane strain ($\sim \xi/R$) is first order in bending amplitude and may play an important role, even for small bending deformations, depending on the relative magnitude of the elastic moduli. This leads to a reduced flexibility of inextensible curved plates due to in-plane stretch and shear [2,8]. This effect vanishes when $R \rightarrow \infty$.

Deformation resulting from the application of a local force perpendicular to the membrane plane is a striking example of this coupling between in-plane stretch and shear and out-of-plane bending [2,8,9]. A buckling instability of the vesicle membrane has been predicted, as for a macroscopic shell, in the limit of very flexible and inextensible membrane [2]. It occurs when it becomes more favorable energetically to concentrate the in-plane stress due to the bending within a narrow ring, centered on the force application point, than to bend and stretch a large piece of membrane around this point. Such instabilities have been studied experimentally and theoretically at a macroscopic scale [10]. We report an observation of such an instability in self-assembled biopolymer and lipid membrane complexes, upon application of a minute force exerted by a micrometer bead displaced with optical tweezers.

Micromechanical experiments [11] have been performed on various cell membranes. Nonlinearities that are sometimes observed [12] may have complicated origins, such as the coupling between membrane and cytosol properties. Few simple membranes with finite shear modulus have been created and studied *in vitro.* Examples to date include lipid vesicles below the lipid melting temperature [13], graphite oxide membranes [14], and the red blood cell skeleton [15]. We have recently tailored new microstructures by self-assembly of actin filaments and fluid unilamellar lipid vesicles (~ 20 μm diameter) [16]. A cross-linked network of actin filaments (mesh size $m \sim 0.1$ μm), thick (thickness $h \sim 0.1$ μm) compared with a bare lipid membrane, is biochemically bound to the outer leaflet of vesicles [Fig. 1(a)]. These membrane exhibit a viscoelastic behavior at high frequency (f): above a few tens of Hz, μ and κ scale as f^z, with $z \approx 0.75$ [16].

Mechanical properties of these microstructures are measured using two beads grabbed with optical tweezers and bound to a vesicle via biotin-streptavidin bonds [Fig. 1(b)]. Strong trapping of the first bead prevents large-scale motion of the liposome. The optical tweezers [Fig. 1(c)] allow one to apply pico-Newton forces on the second bead to deform at low frequency (0.5 to 5 Hz) the membrane locally, either in its plane or perpendicular to it, with a controlled amplitude. Its time position is measured by forming an image of the bead with a He:Ne laser onto a two-quadrant photodiode [Fig. 1(c)]. Depending on its orientation, either in-plane (parallel to the surface) or out-of-plane (perpendicular) motion is measured.

Figure 2 shows the results obtained while imposing on the optical trap a triangular displacement $A_t \sim 310$ nm (peak to peak amplitude) within the membrane plane. In the presence of the actin layer, the probe bead exhibits a triangular displacement of smaller amplitude $A_b \sim 230$ nm. Similar experiments (data not shown) on fluid vesicles show no amplitude drop. Therefore, the actin-coated membrane exerts an elastic force f on the bead. The balance of

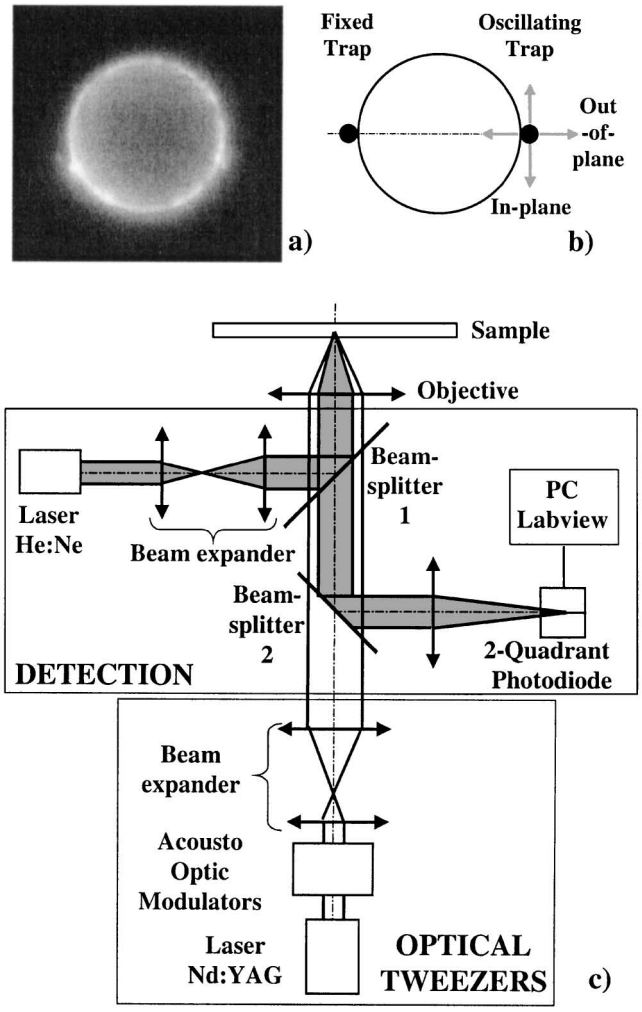

FIG. 1. (a) Vesicles (15 μm diam) coated with actin filaments labeled with Rhodamin-Phalloidin observed by fluorescence microscopy. (b) Principle of the measurement. Two beads are bound to the vesicle using optical tweezers. A first trap maintains the vesicle fixed. The second bead is displaced in a direction parallel to the membrane contour (in-plane) or perpendicular to it (out-of-plane) according to a triangular oscillation. (c) Schematic of the optical tweezers and single-particle tracking experiments. The optical tweezers setup is described in Ref. [16]. An image of the bead is formed on a two-quadrant photodiode with the back-scattered light coming from a He:Ne laser fixed in space and weakly focused on the bead. The differential voltage of the photodiode is proportional to the bead position. The position measurement is calibrated by moving with a piezoelectric stage a bead bound to a glass coverslip (the calibration is linear for amplitudes as large as ± 500 nm). Laser trap displacements are calibrated by moving a trapped bead at low frequency (0.5 Hz) and high laser power (the drag force is negligible). We obtain a 20 nm resolution within the frequency range used.

forces due to the tweezers (trap stiffness $k \sim 10^{-5}$ N/m) and the membrane shear modulus μ [13,16–18] means that $k\ (A_t - A_b) \sim B\ \mu\ A_b$, where B is a numerical constant of order $4\pi/[1 - \ln(R_b/\pi R_\nu)]$ [17], and R_b and R_ν are, respectively, the bead and the vesicle radii. Therefore B is of the order of 4 and μ is approximately 10^{-6} N/m,

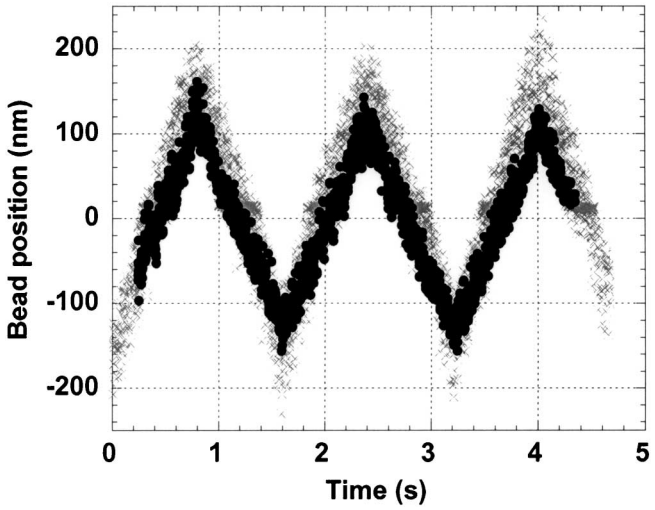

FIG. 2. In-plane oscillations of a 3.1 μm bead attached to an actin-coated membrane (•). To compare, the motion of a trapped bead in solution is also shown (×). In both cases, the laser trap (stiffness $k \sim 10^{-5}$ N/m) was moved at 0.6 Hz according to a triangular wave of amplitude 310 nm. The bulk viscous drag is negligible (it corresponds to a 11 fN force and to a 5 nm displacement of the bead in the trap potential well). The difference in amplitude between the two curves is due to the in-plane shear modulus μ of the actin-coated membrane.

consistent with the known values of bulk shear modulus $G_0(\mu \sim G_0 h)$ of actin filaments solutions, of the order of 0.1 to 10 Pa, depending on the concentration and the reticulation rate [19].

A more striking feature is evidenced in Fig. 3, as the bead is displaced perpendicular to the membrane. As long as the bead is moved a distance smaller than some threshold [Figs. 3(a) and 3(b)], the bead displacement follows linearly the trap position. The reduced amplitude A_b of the triangular displacement of the bead compared to the optical trap one A_t, indicates, as above, that the membrane exerts an elastic force on the bead, characterized by a spring constant k_m. Knowing the trap stiffness $k = 4.5\ 10^{-6}$ N/m, one gets an estimate of k_m: $k_m \sim k(A_t - A_b)/A_b \sim 3\ 10^{-6}$ N/m.

For a larger displacement of the bead, an instability is observed when the bead moves towards the inside of the vesicle: the bead jumps abruptly towards the center of the vesicle. This instability is reversible and reproducible when the bead is further moved in and out of the vesicle [Fig. 3(c)]. After the instability the bead is positioned more "inside" the vesicle than the laser trap: i.e., the shell pulls the bead towards the inside of the vesicle. From Fig. 3(c) one can estimate the critical deformation $l_c \sim 180$ nm and force $f_c \sim k\ (l_t - l_c) \sim 0.5$ pN at the instability threshold as well as the deformation $l_B \sim 320$ nm and the force $f_B \sim k\ (l_t - l_B) \sim 0.1$ pN above the threshold. This instability is observed systematically in our experiments and the critical length l_c is always of the order of 200 nm. As it is not observed with fluid membranes (data not shown), the instability is a characteristic of these composite membranes with finite shear modulus.

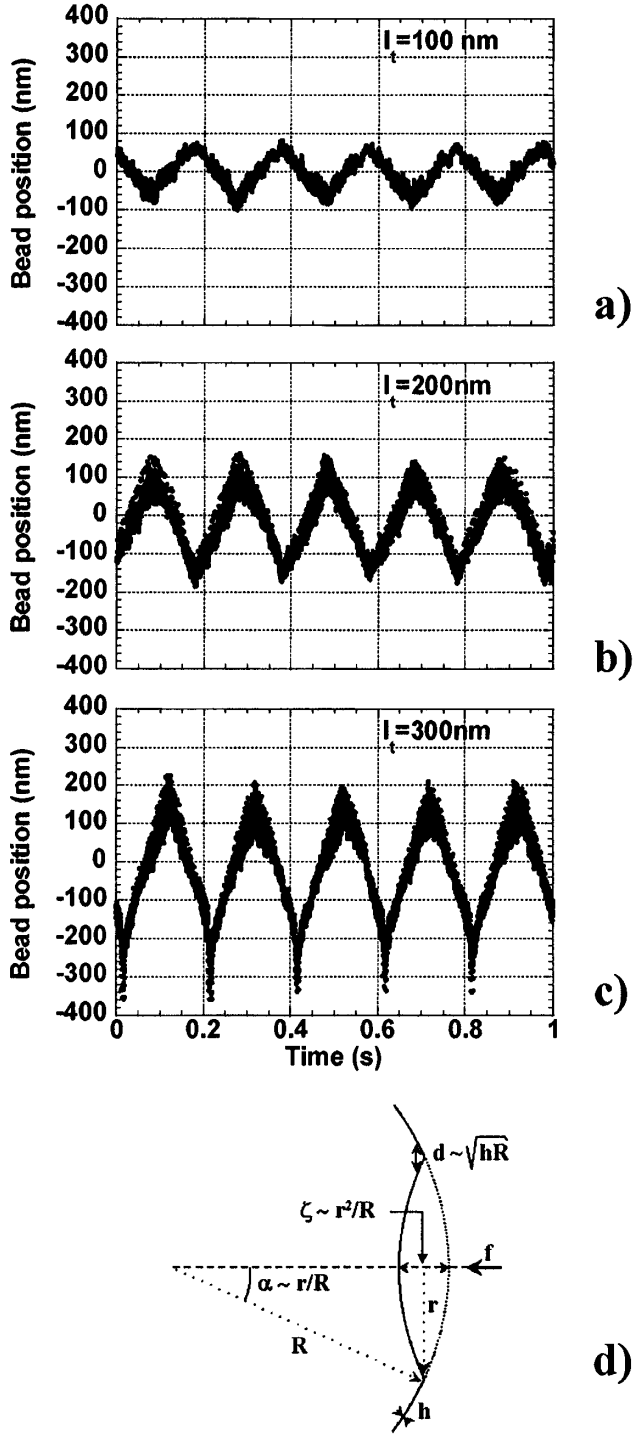

FIG. 3. Out-of-plane oscillations of a 3.1 μm bead attached to an actin-coated membrane. The bead is moved at a frequency of 5 Hz, with a triangular wave of amplitude (a) 100 nm, (b) 200 nm, and (c) 300 nm. The same time scale is used for each curve. The trap stiffness is 4.5 10^{-6} N/m. In (c), the buckling instability is evidenced. (d) Schematic of the membrane shape above the buckling threshold.

We interpret this as a buckling instability of the membrane under the localized force applied by the trapped bead, as described in the introduction [2,8]. Considering the composite membrane as a homogeneous shell of radius R, thickness h, Young modulus E, and Poisson ratio σ, its 2D elastic moduli scale as a function of E, h, and σ as $K = Eh/[2(1 - \sigma)]$, $\mu = Eh/[2(1 + \sigma)]$, and $\kappa = Eh^3/[12(1 - \sigma^2)]$ [8]. The local force applied on the membrane induces some in-plane shear and stretch whose relative magnitudes depend on the exact shape of the deformation and on the respective values of K and μ. For membranes with a finite shear modulus (as, e.g., the red blood cell membrane), the in-plane shear modulus is in general much smaller than the in-plane stretch modulus and pure shear deformations are more energetically favorable [6]. In our case (thick actin-coated membranes and local deformation), the deformation may involve both shear and stretch. Considering an in-plane elastic modulus of the order of Eh, the local force induces, before the buckling threshold [Figs. 3(a) and 3(b)], a bending deformation of amplitude ζ, which extends over a distance d. The in-plane strain being of the order of ζ/R and the local mean curvature of the order of ζ/d^2, the bending energy F_b and the in-plane elastic energy F_s for the deformed surface of area d^2, scale as [2,8]

$$F_b \sim \kappa(\zeta/d^2)^2 d^2 \sim Eh^3\zeta^2/d^2$$

and

$$F_s \sim Eh(\zeta/R)^2 d^2. \quad (1)$$

Minimizing the total free energy F [20] with respect to d leads to $d \sim (\kappa/Eh)^{1/4} R^{1/2} \sim (hR)^{1/2}$ and

$$F = F_b + F_s \sim \kappa\zeta^2/hR \sim Eh^2\zeta^2/R\,. \quad (2)$$

The relation between the applied force f and the deformation amplitude ζ is obtained by comparing the total energy and the work $f\zeta$ exerted by the force f:

$$\zeta = A_0 fhR/\kappa \sim fR/Eh^2, \quad (3)$$

where A_0 is a constant that depends on the Poisson ratio σ. This equation shows that the membrane acts effectively as a linear spring of stiffness k_m given by

$$k_m = f/\zeta \sim \kappa/A_0 Rh\,. \quad (4)$$

If one takes into account only shear (respectively, stretch) deformations, one gets $A_0 = [6(1 - \sigma) + 1]^{-1}$ (respectively, $[6(1 + \sigma) + 1]^{-1}$). As we don't know precisely σ, we can only estimate roughly the bending rigidity from Eq. (4), taking $R \sim 10$ μm, $h \sim 0.1$ μm, and A_0 of order 0.1 to 1 ($0 < \sigma < 1$). This leads to κ of order 100 to $1000 k_B T$. This value is much larger than typical bending moduli of pure lipid membranes ($10-20 k_B T$ [21]) and is consistent with our estimate obtained from analysis of the membrane thermal fluctuations [16]. Consistently, the bending modulus of the actin layer (thickness h and mesh size m) is at least (assuming no cross-linking) of order: $\kappa \sim k_B T\, L_p\, h/m^2 \sim 100 k_B T$, where $L_p \sim 10$ μm is the persistence length of the actin filaments [22].

For large enough force f, a shape change of the shell may happen [2,8], which results in a strong in-plane stretch and shear of the membrane over a narrow "ring" of radius r and size d [Figs. 3(c) and 3(d)]. The bent region

around the point of application of the force has now a size r and a deformation amplitude $\zeta_B \sim r^2/R$. Assuming that most of the elastic energy (both in-plane and out-of-plane) is concentrated in the ring, the order of magnitude of the displacement of a point within the ring is dr/R; the in-plane strain is given by $(dr/R)/R$ and the mean curvature is $(dr/R)/d^2$. Then the in-plane elastic energy and the out-of-plane bending energy scale as

$$F_b \sim \kappa(r/dR)^2 rd \sim Eh^3 r^3/(dR^2)$$

and

$$F_s \sim Eh(rd/R^2)^2 rd \sim Ehr^3 d^3/R^4. \quad (5)$$

Minimizing the total free energy F with respect to d, we obtain $d \sim (hR)^{1/2}$ and

$$F \sim Er^3(h/R)^{5/2} \sim Eh^{5/2}{\zeta_B}^{3/2}/R\,. \quad (6)$$

Comparing Eqs. (2) and (6), the buckling takes place typically for a deformation $\zeta_B \sim h$. In our experiments, the typical deformation at the buckling threshold is indeed of order 200 nm, or approximately the membrane thickness. Finally, the buckling instability is totally reversible, which shows that no plastic deformation takes place.

To conclude, self-assembled actin-coated membranes are characterized by an in-plane shear-modulus μ around 10^{-6} N/m and large bending modulus κ of a few $100k_BT$. We have shown the first clear evidence of a buckling instability when a force is applied locally perpendicular to the membrane plane. This instability presumably comes from the coupling between out-of-plane deformation and in-plane strain, which is the origin of many of the interesting properties of polymerized, tethered, and solid membranes.

We thank Thomas Duke for helpful advice. F. C. M. was supported by the CNRS, the National Science Foundation, and the Whitaker Foundation. This work was supported in part by Fondation pour la Recherche Médicale.

*Present address: Van der Waals-Zeeman Instituut, Universiteit van Amsterdam, Amsterdam, The Netherlands
†Corresponding author.
Email address: bourdieu@ldfc.u-strasbg.fr
‡Present address: Division of Physics & Astronomy, Vrije Universiteit, Amsterdam, The Netherlands

[1] Y. Kantor, M. Kardar, and D. R. Nelson, Phys. Rev. Lett. **57**, 791 (1986); J. A. Aronovitz and T. C. Lubensky, Phys. Rev. Lett. **60**, 2634 (1988); E. Guitter *et al.,* Phys. Rev. Lett. **61**, 2949 (1988).
[2] H. Yoon and J. M. Deutsch, Phys. Rev. E **56**, 3412 (1997).
[3] D. Moldovan and L. Golubovic, Phys. Rev. E **60**, 4377 (1999).
[4] For a review, see U. Seifert, Adv. Phys. **46**, 13 (1997).
[5] F. Brochard and J. F. Lennon, J. Phys. (Paris) **36**, 1035 (1975).
[6] E. Evans, R. Waugh, and L. Melnik, Biophys. J. **16**, 585 (1976); E. Evans, Biophys. J. **16**, 597 (1976).
[7] B. Alberts *et al., Molecular Biology of the Cell* (Garland, New York, 1994).
[8] L. Landau and E. Lifchitz, *Théorie de l'élasticité* (Mir, Moscow, 1967).
[9] A. A. Boulbitch, Phys. Rev. E **57**, 2123 (1998).
[10] L. Pauchard and S. Rica, Philos. Mag. B **78**, 225 (1998); A. Boudaoud *et al.,* Nature (London) **407**, 718 (2000), and Refs. [3–8] therein.
[11] S. Hénon *et al.,* Biophys. J. **76**, 1145 (1999); A. R. Bausch *et al.,* Biophys. J. **75**, 2038 (1998); A. A. Garcia, W. C. Petitgrew, and J. Graham, Scanning Microsc. **7**, 577 (1993); M. Arnoldi *et al.,* Phys. Rev. E **62**, 1034 (2000).
[12] J. Sleep *et al.,* Biophys. J. **77**, 3085 (1999).
[13] R. Dimova, B. Pouligny, and C. Dietrich, Biophys. J. **79**, 340 (2000).
[14] X. Wen *et al.,* Nature (London) **355**, 427 (1992); M. S. Spector *et al.,* Phys. Rev. Lett. **73**, 2867 (1994).
[15] C. F. Schmidt *et al.,* Science **259**, 952 (1993).
[16] E. Helfer *et al.,* Phys. Rev. Lett. **85**, 457 (2000); E. Helfer *et al.,* Phys. Rev. E **63**, 021904 (2001).
[17] A. E. H. Love, *A Treatise on the Mathematical Theory of Elasticity* (Dover, New York, 1944).
[18] A. A. Boulbitch, Phys. Rev. E **59**, 3402 (1999).
[19] P. A. Janmey *et al.,* J. Biol. Chem. **269**, 32503 (1994); A. Palmer *et al.,* Biophys. J. **76**, 1063 (1999); B. Schnurr *et al.,* Macromolecules **30**, 7781 (1997).
[20] We do not take into account an additional energy term that comes from the incompressibility of the fluid inside the vesicle. Since the fluid cannot exchange through the membrane at the time scale of the experiment [see K. Olbrich *et al.,* Biophys. J. **79**, 321 (2000)], the whole vesicle membrane is stretched when the force is applied. For the deformation of amplitude ζ extending over an area $d^2 \sim hR$, the area increase (of the membrane of total area A) is $\delta A \sim 2\zeta d^2/R$ and the additional stretching energy scales as $Eh(\delta A/A)^2 A \sim Eh\zeta^2 d^4/R^4 \sim F_S(d/R)^2 \ll F_s$.
[21] E. A. Evans and W. Rawicz, Phys. Rev. Lett. **64**, 2094 (1990).
[22] A. Ott *et al.,* Phys. Rev. E **48**, 1642 (1993).